U(1) lattice gauge theory in the electric-field representation

S. E. Koonin, E. A. Umland,* and M. R. Zirnbauer
W. K. Kellogg Radiation Laboratory, California Institute of Technology, Pasadena, California 91125
(Received 16 September 1985)

The Hamiltonian formulation of U(1) lattice gauge theory is studied in a basis of eigenstates of the electric-field operator. The guided-random-walk algorithm of Chin *et al.* is transcribed to the electric-field basis, and exact ground-state properties of the theory in three space dimensions are calculated. A novel variational scheme is used to compute the potential between two static charges for two space dimensions.

I. INTRODUCTION

Lattice gauge theories are, at present, the most promising method for extending the successes of quantum chromodynamics from the perturbative regime of deep-inelastic scattering to the nonperturbative phenomena of hadron structure and interactions. The most common approach to these theories is through a Lagrangian formulation, where the action, a functional of the gluon and quark fields, is discretized on a four-dimensional Euclidean space-time lattice and the observables are evaluated by a Monte Carlo sampling of space-time histories.[1] This approach has had a number of successes, including calculations of the interquark potential and the quark-gluon plasma, as well as a rough description of meson and baryon properties.[2,3]

Despite the considerable progress which has been (and continues to be) made through the Lagrangian formulation of lattice gauge theory, the approach has some undesirable features. Foremost among these is that the sampling over histories is biased only by the action, and there is no opportunity for using physical constraints (e.g., quarks cluster into hadrons, a flux tube connects a quark and an antiquark) to improve the efficiency of the sampling algorithm. Indeed, statistical precision is currently the main limitation in many Lagrangian calculations of QCD phenomena and this problem will become even more apparent as one attempts first-principles descriptions of the multinucleon systems of interest in nuclear physics.

The Hamiltonian formulation,[4] less often pursued, offers an alternative to the Lagrangian framework with several attractive features. Here, the fields are discretized on a three-dimensional spatial lattice and the essential task is to find the ground state of a Hamiltonian that is a differential operator in the field variables. The problem thus has the appearance of a conventional "many-body" (actually, many-variable) system and an arsenal of familiar techniques can be called into service. These include variational methods, expansion in a truncated basis, and exact Green's function or path-integral Monte Carlo methods, all of which have the advantage of allowing the use of a well-chosen trial wave function to improve greatly the precision and efficiency of the calculation.

Although Hamiltonian methods have been used extensively to treat nonrelativistic many-body systems, there have been relatively few attempts to apply them to lattice gauge theories. The first numerical Hamiltonian calculations were done by Chin *et al.*,[5,6] by Heys and Stump,[7,8] and by DeGrand and Potvin,[9] who treated the U(1) and SU(2) pure-gauge vacua with variational and exact Monte Carlo methods. Diagonalization in a well-chosen basis has been performed by Duncan and Roskies.[10]

In this paper, we are concerned with the application of Hamiltonian methods to the electric-field representation of lattice gauge theories. The basic dynamic variables defining the electric-field representation are the fluxes of electric field along the links of the lattice. For many purposes, these variables are more convenient to work with than are the vector potential variables commonly used. Two distinct calculations will be discussed here. First, we calculate the ground state of U(1) lattice gauge theory in $d = 3$ space dimensions by adapting the guided random walk algorithm of Ref. 5 to the electric-field representation. Second, we calculate the potential between two static charges [again for the U(1) theory, but in 2 space dimensions]. The latter is done in a variational framework, in which choices are made not only for the vacuum wave function, but also for the fluctuations of the flux tube between the charges (or "quarks"). Although the first calculation has no obvious extension to the non-Abelian case, the second does.

The balance of this paper is organized as follows. In Sec. II we review the Hamiltonian formulation of the U(1) theory in the vector potential basis. Particular attention is given to the gauge transformation properties of the eigenstates and the interpretation of the interquark potential as an excitation energy. In Sec. III we discuss the problem in the electric-field basis, which has the advantage that the wave functions of interest are real and positive in this representation. We also discuss the familiar independent-plaquette wave function in this language and introduce an independent-link wave function. In Sec. IV we formulate the method of guided random walks in the electric-field basis, and present our numerical results for the ground state of U(1) in $d = 3$ dimensions. Formalism and numerical results for the interquark potential in $d = 2$ dimensions are presented in Sec. V, and we conclude with a discussion of future prospects in Sec. VI.

II. HAMILTONIAN FORMULATION OF THE INTERQUARK POTENTIAL

The Hamiltonian for U(1) lattice gauge theory has been derived by several authors[11–13] and we only state the result here. After a suitable scaling, the system in d spatial dimensions ($d = 2, 3$) is described by an angular variable, $0 \le \phi_l < 2\pi$, on each of the dL^d links l of an L^d spatial lattice with periodic boundary conditions. The Hamiltonian is

$$H = -\frac{1}{2}\sum_l \frac{\partial^2}{\partial\phi_l^2} + \lambda \sum_p (1 - \cos\psi_p) , \tag{2.1}$$

where the sum in the second term runs over all elementary plaquettes p, ψ_p is the directed sum of the ϕ_l on the four links of the plaquette, and $\lambda \equiv g^{-4}$ is related to the coupling constant g. In the physical weak-coupling limit, this theory reduces to ordinary electrodynamics, with ϕ_l being proportional to the vector potential, $-i\partial/\partial\phi_l$ being proportional to the electric flux along the link l, and ψ_p being proportional to the magnetic flux through the plaquette p. The first term in (2.1) can thus be identified as the energy stored in the electric field, while the second is the magnetic energy.

There are, of course, infinitely many eigenstates of H, each of them a different function of the dL^d link variables ϕ_l. However, the gauge invariance of H provides L^d constants of the motion by which these eigenstates can be classified. In particular, for each lattice site s, the operator

$$(\nabla\cdot E)_s \equiv \sum_{l\in s} (-)^{\epsilon_l} \frac{1}{i}\frac{\partial}{\partial\phi_l} , \tag{2.2}$$

is easily seen to commute with H. Here, the sum is a directed one over the $2d$ links touching s; i.e., $(-)^{\epsilon_l}$ is $+1$ for the links emanating from s in the positive sense, and -1 otherwise. The eigenstates of H can therefore be classified by the eigenvalues associated with these operators, and H is diagonal with respect to these quantum numbers. Note that since the eigenvalues of $-i\partial/\partial\phi_l$ are integers (recall that ϕ_l is an angular variable), the eigenvalues of $(\nabla\cdot E)_s$ are also integers; they are the amount of charge at each site of the lattice.

The vacuum state of the theory, $\Psi_0(\phi)$, is the lowest-energy eigenstate of H in the subspace of Hilbert space that has no charge on any of the lattice sites. That is, it is a state that is annihilated by each of the operators (2.2), a property sometimes referred to as Gauss's law. Similarly, the lowest-energy state in the subspace having charges of $+1$ at site a and -1 at site b, $\Psi_{q\bar{q}}$, is annihilated by all of the operators (2.2), except by those for sites a and b, whose eigenvalues are $+1$ and -1, respectively. The difference between the energy of this state and that of the vacuum is the potential between the static quark and static antiquark.

Further insight into the $q\bar{q}$ state can be had by considering a specific component of the wave function. It is easy to verify that the state

$$\Phi_{q\bar{q}} = P_+\Phi_0, \qquad P_+ = \prod_a^b e^{\pm i\phi_l} , \tag{2.3}$$

has the proper gauge transformation properties. Here, the product is over *any* path on the lattice connecting site a and b (the sign for a given link l in the exponent being determined by the direction in which the path traverses the link), and Φ_0 is any state in the vacuum (or chargeless) subspace, perhaps even the vacuum itself. This state corresponds to a "string" of unit electric flux running from a to b on the path chosen. Of course, the exact eigenstate $\Psi_{q\bar{q}}$ might involve a coherent superposition of many such states. Still, the form of (2.3) does show that the wave function of the $q\bar{q}$ state is intrinsically complex in the vector potential basis, an unattractive feature if Monte Carlo methods are to be applied. It is therefore more convenient to work in the canonically conjugate electric-field basis, to which we now turn.

III. THE ELECTRIC-FIELD REPRESENTATION

To formulate U(1) lattice gauge theory, we need to choose a complete set of basis states in which to represent the Hamiltonian and its eigenfunctions. One such set are the eigenstates of the vector potential A defined on the links of the lattice ($\propto \phi_l$) as discussed in the previous section. Alternatively, the eigenstates of the electric field E can be used. Because the electric field is canonically conjugate to the vector potential, the corresponding representation is analogous to the familiar momentum representation in single-particle quantum mechanics.

For our purposes, the electric-field, or E, representation offers two potential advantages over the vector potential, or A, representation.

(1) The degrees of freedom in the E representation are integers because the variables ϕ_l have a compact range, $0 \le \phi_l < 2\pi$. A particular electric-field configuration is represented as a collection of integers, one for each link. The numerical advantages of integer arithmetic on the computer are well known and have prompted the use of discrete subgroups in lattice gauge theory calculations.[14] The E representation has these same advantages and is free of approximations.

(2) The physics of the $q\bar{q}$ state is more transparent in this representation, and the wave function describing the state is real and positive. The strong-coupling ($\lambda \to 0$), or confining, limit of this state is a line of unit electric flux between the charges superimposed on the strong-coupling vacuum, while the weak-coupling ($\lambda \to \infty$) limit is expected to reduce (for $d = 3$) to the classical electric dipole field at large distances from the charges.

The electric-field representation is introduced by making a Fourier expansion of the wave function $\Psi = \Psi(\phi)$:

$$\Psi(\phi) = \sum_n \langle \phi \mid n \rangle \Psi(n) ,$$
$$\langle \phi \mid n \rangle = \exp\left[i \sum_l n_l \phi_l \right] . \tag{3.1}$$

Here, n denotes a configuration of integers n_l, and $\Psi(n)$ are the components of the wave function in the new representation. Gauge-invariant states can be expressed in terms of basis states $\langle \phi \mid n \rangle$ that satisfy Gauss's law, $(\nabla\cdot n)_s = 0$. (The subscript s indicates that the lattice

divergence is evaluated on sites.) For some purposes, it is useful to satisfy the gauge constraint $(\nabla\cdot n)_s = 0$ explicitly by introducing plaquette variables m_p via the relation

$$n_l = (\nabla \times m)_l \ . \tag{3.2}$$

The gauge invariance of basis states $\langle \phi \mid n \rangle$ with n given by Eq. (3.2) is evident from

$$\exp\left[i \sum_l n_l \phi_l\right] = \exp\left[i \sum_l (\nabla \times m)_l \phi_l\right] = \exp\left[-i \sum_p m_p (\nabla \times \phi)_p\right] \tag{3.3}$$

since the last expression depends on ϕ_l only through the (dimensionless) gauge-invariant magnetic field $\psi_p = (\nabla \times \phi)_p$.

It is important that Eq. (3.2) does not determine the m_p uniquely. In $d=3$ space dimensions, we can generate from a given solution m_p another solution $m_{p'}$ by adding the gradient of an arbitrary field σ (defined on cubes): $m_{p'} = m_p + (\nabla\sigma)_p$. In contrast, for $d = 2$ the solution of Eq. (3.2) is unique if free boundary conditions are used, and is unique within an overall additive constant if periodic boundary conditions are used.

It is crucial to make a very clear distinction between two different electric-field bases. On the one hand, the transformation coefficients $\langle \phi \mid n \rangle$ in Eq. (3.1) define what we call the "n basis." This basis is orthogonal, $\langle n' \mid n \rangle = \delta_{n'n}$, and complete in the *total* Hilbert space. As has already been said, restriction to the gauge-invariant subspace is made by *imposing* Gauss's law. On the other hand, the set of functions

$$\langle \phi \mid m \rangle \equiv \exp\left[-i \sum_p m_p \psi_p\right] , \tag{3.4}$$

defined in terms of plaquette variables $m_p = 0, \pm 1, \pm 2, \ldots$, is referred to as the "m basis." This basis has the advantage that gauge invariance is automatically satisfied. However, for $d = 3$ the m basis is actually *overcomplete* (and thus *nonorthogonal*) in the gauge-invariant subspace. This follows from the fact that two states $\mid m \rangle$ and $\mid m' \rangle$ have an overlap of unity if the respective configurations m_p and $m_{p'}$ differ only by a gradient:

$$\langle m' \mid m \rangle = \int d[\phi] \exp\left[-i \sum_p (m_p - m_{p'}) \psi_p\right] = \int d[\phi] \exp\left[i \sum_p (\nabla\sigma)_p (\nabla \times \phi)_p\right] = \int d[\phi] = 1 \ . \tag{3.5}$$

(Here, $d[\phi] \equiv \prod_l d\phi_l / 2\pi$.) Eq. (3.5) is just another way of saying that two sets m_p and $m_{p'}$ which differ only by a gradient *describe the same physical state.*

It is therefore clear that some care must be exercised when using the m basis in practical calculations (for $d = 3$). For example, due to the vast overcompleteness, many states in the m basis are spurious, making it necessary to project in some exact or approximate manner onto the physical subspace. Alternatively, one might attempt to make the m basis less redundant by imposing additional constraints. One possibility is to consider only sets m that are purely transverse. Unfortunately, the implementation of such a condition requires highly nonlocal operations, which are unattractive from a computational point of view. For these and other reasons, most numerical calculations discussed in this paper have been performed using the n basis. (We note in passing that variational and exact m basis calculations have been carried out by Heys and Stump.[7,8] These authors, however, do not discuss the problem of nonorthogonality of the m basis. In fact, they claim[8] that there exists a one-to-one correspondence between m configurations and sets of closed loops of electric flux on the lattice; the analysis presented above shows this to be incorrect. We believe that this, and not the trapping of the system in some "metastable phase," is responsible for the problems they encounter when using the mean-plaquette wave function.[7])

We now turn to the representation of the Hamiltonian in the electric-field basis (n basis). The matrix element of H between two states $\mid n \rangle$ and $\mid n' \rangle$ is evaluated as

$$\langle n' \mid H \mid n \rangle = \int d[\phi] \exp\left[-i \sum_l n_l' \phi_l\right] \left[-\frac{1}{2} \sum_l \frac{\partial^2}{\partial \phi_l^2} + \lambda \sum_p (1 - \cos\psi_p)\right] \exp\left[i \sum_l n_l \phi_l\right] = \frac{1}{2}\left[\sum_l n_l^2\right] \delta_{n',n} + \lambda \sum_p \left(1 - \tfrac{1}{2}\delta_{n',n+l_p} - \tfrac{1}{2}\delta_{n',n-l_p}\right) . \tag{3.6}$$

Here, $n + l_p$ ($n - l_p$) denotes the configuration that is obtained by incrementing (decrementing) n by one unit in a directed sense simultaneously on all four links contained in the plaquette p. Repeated action of $\langle n' \mid H \mid n \rangle$ on a configuration n leaves $(\nabla\cdot n)_s$ invariant, which is equivalent to saying that H is gauge invariant. We also note that the association of "kinetic" and "potential" energies with the electric and magnetic parts of the Hamiltonian is reversed in going from the A to the E representation. In particular, the magnetic term now has a form reminiscent of a discrete second derivative.

Many calculations that have been performed in the vector potential representation are based on the independent-plaquette vacuum trial state

$$\Phi(\phi)=\prod_p f(\psi_p)=\prod_p \exp(\beta\cos\psi_p)\ . \tag{3.7}$$

To transform this state to the E representation we expand in terms of Fourier components:

$$\Phi(\phi)=\prod_p\left[\sum_{m_p} I_{m_p}(\beta)\exp(-im_p\psi_p)\right]$$
$$=\sum_m\left[\prod_p I_{m_p}(\beta)\exp(-im_p\psi_p)\right], \tag{3.8}$$

where the $I_{m_p}(\beta)$ are modified Bessel functions of order m_p. Multiplication with $\langle\phi\,|\,n\rangle^*$ and integration over all ϕ_l gives the n basis representation of Φ:

$$\Phi(n)=\sum_m\int d[\phi]\exp\left[-i\sum_l n_l\phi_l\right]\left[\prod_p I_{m_p}(\beta)\right]$$
$$\times\exp\left[-i\sum_p m_p\psi_p\right]$$
$$=\sum_m\left[\prod_p I_{m_p}(\beta)\prod_l\delta[(\nabla\times m)_l-n_l]\right]. \tag{3.9a}$$

On the other hand, if we are willing to work in the nonorthogonal m basis, then Φ takes the much simpler product form

$$\Phi(m)=\prod_p I_{m_p}(\beta)\ . \tag{3.9b}$$

Equation (3.9a) means that, to evaluate the amplitude $\Phi(n)$ for a given configuration n, we must sum over all m that describe the physical state defined by n. It is not computationally feasible, in general, to calculate this sum exactly for every configuration. The situation simplifies in the strong-coupling limit (β sufficiently small), where individual terms in the sum correspond to different powers in β. For the simple case of zero electric field everywhere, let us examine in $d=3$ the plaquette geometries represented by the various terms. The first, the "minimal set," is merely all $m=0$. The next is a cube of six excited plaquettes with the values of the three whose outward normals point in the positive direction equaling $+1$ (or -1) and the others equaling the opposite (see Fig. 1). A single such cube is suppressed relative to the minimal term by β^6. Higher terms represent larger closed volumes and/or larger values of m variables and are suppressed even further. It is thus permissible to retain only the minimal set in the sum over m for small values of β. For a general configuration n, finding the corresponding minimal set amounts to determining the minimal surface that has the flux lines defined by n as boundaries. Unfortunately, finding the minimal surface for a general electric-field configuration is a nontrivial numerical problem, and the trial state (3.9a) is therefore quite difficult to deal with in practice. The situation is of course different for $d=2$. In this case, the minimal surface is trivially given, and Eq. (3.9a) collapses to a sum of terms which differ only by a constant over the entire lattice, so that higher-order terms are suppressed at least as β^V, where $V=L^2$ is the total number of plaquettes (the area of the lattice).

As another choice for the vacuum trial state, we can define an "independent-link" wave function:

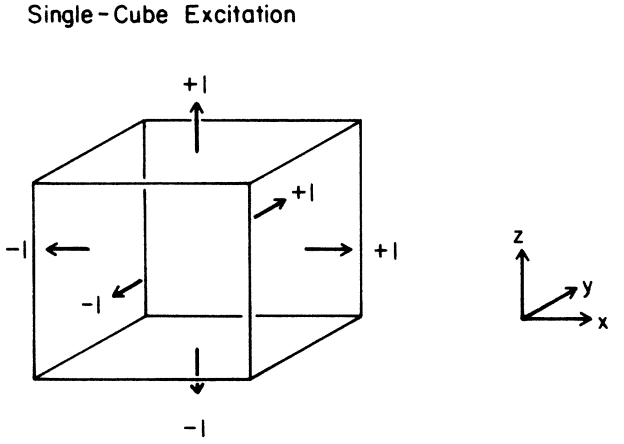

FIG. 1. Values of the plaquette variables m for a single excited cube. This excitation is spurious as it leaves the integers n (electric-field strengths) unchanged.

$$\Phi(n)=\prod_l I_{n_l}(\beta)\prod_s\delta[(\nabla\cdot n)_s]\ , \tag{3.10}$$

where gauge invariance of the state is imposed by requiring $(\nabla\cdot n)_s=0$. This wave function contains long-range correlations between plaquette variables as is seen by transforming back to the A representation (see the Appendix). For large values of β the result in $d=3$ is given by

$$\Phi(\phi)\simeq\exp\left[-\frac{\beta}{2}\sum_{pp}{}'\frac{\psi_p\psi_{p'}}{|p-p'|}\right], \tag{3.11}$$

with $|p-p'|$ the distance between the two plaquettes. While a wave function of the form (3.11) is quite difficult to handle numerically, in the E representation, Eq. (3.10), the algorithm is relatively straightforward.

IV. GUIDED RANDOM WALKS IN THE ELECTRIC-FIELD REPRESENTATION

In this section, we calculate the ground-state energy for the U(1) theory as a function of λ on a 4^3 lattice and compare with earlier work in the A representation.[5] We use as trial states both the independent-link and the independent-plaquette wave functions described in the previous section. Variational as well as time-evolved exact ground-state energies are evaluated.

A. Variational calculations

Given a trial wave function $\Phi(n)$, we generate electric-field configurations n distributed according to $\Phi^2(n)$ via the Metropolis Monte Carlo method.[15] The variational energy, or expectation value of the Hamiltonian in the state Φ, is computed by averaging the local energy density $\Phi^{-1}(n)(H\Phi)(n)$ over these configurations,

$$E_V=\frac{1}{Z}\sum_{i=1}^{Z}\Phi^{-1}(n_i)(H\Phi)(n_i)\ , \tag{4.1}$$

where E_V is subject to statistical error for finite Z. Both

the Metropolis updating procedure and Eq. (4.1) are straightforward to implement numerically when an independent-link wave function, Eq. (3.10), is chosen for Φ. [The only subtlety involved is the necessity of preserving gauge invariance. This is accomplished by simultaneously updating all links l belonging to a given plaquette p according to $n_l' = n_l + (\nabla \times \delta m)_l$ with $\delta m_p = \pm 1$.] For the independent-plaquette wave function (3.9a), however, we encounter the difficulties discussed in the previous section. It is therefore preferable to work in the m basis in this case. Since $\langle m \mid m + \nabla\sigma \rangle = 1$ for arbitrary m and σ, the overlap integral in the m basis is given by

$$\langle \Phi \mid \Phi \rangle = \sum_{m,\sigma} \Phi(m)\Phi(m+\nabla\sigma) . \tag{4.2}$$

Using this relation we can write the variational energy as

$$E_V = \sum_{m_1,\sigma} \left[\sum_{m_2} \Phi(m_2)\langle m_2 \mid H \mid m_1 \rangle \Phi^{-1}(m_1) \right] \times \frac{\Phi(m_1)\Phi(m_1+\nabla\sigma)}{\sum_{m',\sigma'} \Phi(m')\Phi(m'+\nabla\sigma')} . \tag{4.3}$$

The calculation now proceeds by making Metropolis moves on both m and σ according to the weight function $\Phi(m)\Phi(m+\nabla\sigma)$ and then averaging the expression in large parentheses over the configurations generated in this way. The coding is simplest for the independent-plaquette wave function (3.9b), but other choices are possible. In particular, the independent-link wave function (3.10) or, for that matter, any combination of independent-plaquette and independent-link wave functions, can be treated using Eq. (4.3).

We present variational ground-state energies, and energies calculated from the strong-coupling expansion (SCE),[5] corresponding to values of λ in the strong, intermediate, and weak-coupling regimes in Table I. The independent-plaquette wave function is known to approach the exact ground state as $\lambda \to 0$. In this regime, the independent-plaquette state gives indeed a lower energy than the independent-link wave function. On the other hand, the independent-link wave function is superior in the intermediate and weak-coupling regions. This we attribute to the presence of plaquette-plaquette correlations, which are missing in the independent-plaquette state. It is conceivable that a well-chosen combination of the two gives a good description of the vacuum far into the weak-coupling region.

B. Generating the exact ground state via time evolution

The guided random walk (GRW) algorithm is a numerical method for evolving a given trial state to the exact ground state of a quantum many-body system. In Refs. 5 and 6 this method was applied to U(1) and SU(2) lattice gauge theory in the A representation. Here we show how to formulate the GRW algorithm in a discrete basis and apply it to the U(1) theory in three space dimensions using the electric-field representation.

Consider the product

$$\rho(n,t) = \Phi(n)\Psi(n,t) , \tag{4.4}$$

where, for now, n may stand for *any* set of discrete variables (though eventually n will be identified with electric-flux configurations), and $\Phi(n)$ is the trial or guiding wave function. Let the time evolution of ρ be governed by the (imaginary-time) Schrödinger equation

$$-\frac{\partial}{\partial t}\rho(n',t) = \Phi(n') \sum_n \langle n' \mid (H - E_{\text{norm}}) \mid n \rangle \times \Phi^{-1}(n)\rho(n,t) , \tag{4.5}$$

where $E_{\text{norm}}(t)$ is an as yet unspecified c-number function. If the initial wave function, $\Psi(n,0) \equiv \Phi(n)$, has a nonvanishing overlap with the exact ground state of H, $\Psi_0(n)$, then $\Psi(n,t) \to \Psi_0(n)$ as $t \to \infty$. We split the Hamiltonian into kinetic and potential parts,

$$\langle n' \mid H \mid n \rangle = T(n',n) + V(n)\delta_{n'n} , \tag{4.6}$$

and decompose the kinetic term as follows:

TABLE I. Variational and exact U(1) ground-state energies for a simple cubic lattice of dimension 4^3. The exact results for the independent-plaquette trial function were taken from Chin *et al.* Φ_0^{plaq} = independent-plaquette trial function. Φ_0^{link} = independent-link trial function. β = variational parameter determined by finding minimum energy listed in column 2. SCE = strong-coupling expansion.

	Variational			Exact	
λ	Φ_0^{plaq} (m basis)	Φ_0^{link} (n basis)	SCE	Φ_0^{plaq} (A representation)	Φ_0^{link} (n basis)
0.6	0.5124(3)	0.5308(7)	0.5108	0.509(1)	0.515(2) $\beta = 1.70$
1.0	0.7635(9)	0.7201(3)	0.7523	0.719(1)	0.708(1) $\beta = 2.35$
1.8	1.0754(19)	0.9986(9)	1.0150	0.997(2)	0.982(1) $\beta = 3.20$

$$\Phi(n')T(n',n)\Phi^{-1}(n)\equiv\Phi^{-1}(n)\left[\sum_{n''}T(n,n'')\Phi(n'')\right]\delta_{n'n}+k(n',n)\ ,$$
$$k(n',n)=\Phi(n')T(n',n)\Phi^{-1}(n)-\Phi^{-1}(n)\left[\sum_{n''}T(n,n'')\Phi(n'')\right]\delta_{n'n}\ . \tag{4.7}$$

The Schrödinger equation can now be written as

$$-\frac{\partial}{\partial t}\rho(n',t)=\sum_{n}[k(n',n)+v(n)\delta_{n'n}]\rho(n,t), \tag{4.8}$$

where we have defined

$$v(n)=\Phi^{-1}(n)\left[\sum_{n''}\langle n\mid H\mid n''\rangle\Phi(n'')\right]-E_{\rm norm}\ . \tag{4.9}$$

The GRW algorithm is implemented by exponentiating Eq. (4.8):

$$\rho(n',t+\delta t)=\sum_{n}\langle n'\mid e^{-(k+v)\delta t}\mid n\rangle\rho(n,t)$$
$$=W(n';\delta t)\sum_{n}K(n',n;\delta t)\rho(n,t)+O(\delta t^2)\ , \tag{4.10a}$$

$$K(n',n;\delta t)=\langle n'\mid e^{-k\delta t}\mid n\rangle,\quad W(n;\delta t)=e^{-v(n)\delta t}\ . \tag{4.10b}$$

The generator k, Eq. (4.7), was so constructed as to satisfy

$$\sum_{n'}k(n',n)\equiv 0 \tag{4.11}$$

for *all* n. [Note that the only condition required for (4.11) to hold is the symmetry of T, $T(n,n')=T(n',n)$.] Equation (4.11) means that the kernel $K(n',n;\delta t)$ conserves probability:

$$\sum_{n'}K(n',n;\delta t)\equiv 1\ . \tag{4.12}$$

The action of K on ρ therefore can be simulated by performing a random walk in the space of n variables with $K(n',n;\delta t)$ being the probability for stepping from n to n' in time δt. In practice, since Eq. (4.10a) is correct only to order δt, K is replaced by

$$K(n',n;\delta t)\simeq\langle n'\mid 1-k\delta t\mid n\rangle=\delta_{n'n}-k(n',n)\delta t\ . \tag{4.13}$$

On the computer, the GRW algorithm proceeds as follows.

(1) Choose a time step δt and generate an ensemble of N sets of variables n distributed according to $\Phi^2(n)$.

(2) Random walk each set n according to (4.13).

(3) At each time step, replicate or delete each member n of the ensemble according to the weight $W(n;\delta t)$. At the end of the time step, adjust the normalization energy $E_{\rm norm}$ to keep the population stable. (In the relaxation phase of the time evolution this requirement will tend to cause $E_{\rm norm}$ to decrease with time until $E_{\rm norm}\cong E_0$.)

(4) After the system has relaxed to the ground state (so that the ensemble is distributed according to $\Phi\Psi_0$), continue evolution (thereby generating more statistically independent sets n_i distributed as $\Phi\Psi_0$) to reduce the statistical variance in the observables to be calculated.

(5) The ground-state energy can be computed from

$$E_0=\frac{\langle\Phi\mid H\mid\Psi_0\rangle}{\langle\Phi\mid\Psi_0\rangle}\approx\frac{1}{Z}\sum_{i=T+\delta t}^{T+Z\delta t}\Phi^{-1}(n_i)(H\Phi)(n_i) \tag{4.14}$$

as well as from

$$E_0\cong\frac{1}{Z}\sum_{i=T+\delta t}^{T+Z\delta t}(E_{\rm norm})_i\ , \tag{4.15}$$

where the sum over time steps (and ensemble members at each time step) begins at some time T by which the system has relaxed to the ground state. (Both methods of calculating E_0 should give the same answer within statistical errors as $\delta t\to 0$.)

(6) Repeat the calculation with smaller values of the time step δt and extrapolate to $\delta t=0$.

To apply this algorithm to U(1) lattice gauge theory we interpret n as a configuration of electric fluxes, i.e., as the set of integers n_l on the links of the lattice. The explicit expressions for k and v are then given by

$$\lambda^{-1}k(n',n)=\frac{1}{2}\sum_{p}\left[\frac{\Phi(n+l_p)+\Phi(n-l_p)}{\Phi(n)}\right]\delta_{n'n}-\frac{1}{2}\sum_{p}\left[\frac{\Phi(n+l_p)}{\Phi(n)}\delta_{n',n+l_p}+\frac{\Phi(n-l_p)}{\Phi(n)}\delta_{n',n-l_p}\right], \tag{4.16}$$

$$v(n)=\frac{1}{2}\left[\sum_{l}n_l^2\right]+\lambda\sum_{p}\left[1-\frac{1}{2}\left[\frac{\Phi(n+l_p)+\Phi(n-l_p)}{\Phi(n)}\right]\right]-E_{\rm norm}\ , \tag{4.17}$$

and $\Phi(n)$ is a suitable guiding wave function.

We showed above that variational ground-state energies can be calculated using *either* of the two E representations that were introduced in Sec. III, i.e., the n basis *or* the m basis. In contrast, the exact algorithm just described requires the n basis formulation. The derivation of the method relies in an essential fashion on the orthogonality of the basis, and we have not been able to find a simple

way of relaxing this condition. This limits our choice of guiding wave function to the independent-link state defined in Eq. (3.10), optimized by varying β to minimize E_V defined in Eq. (4.1).

Our results for a 4^3 lattice are given in Fig. 2 and Table I. A comparison with the GRW calculations of the ground-state energy in the A representation[5] is presented in Table I. In our case the GRW algorithm required about 60 VAX 11/750 CPU minutes per δt data point, while the A representation calculations with continuous fields consumed about 2 h.[16]

We notice that at the extrapolated $\delta t = 0$ limit the energy is reduced below the variational energy and the normalization and expectation value energies agree within statistics. At weak coupling ($\lambda = 1.8$), the independent-link guiding wave function appears to give a slightly lower energy than does the independent-plaquette wave function used in the A representation GRW algorithm. The same is observed in the intermediate-coupling region ($\lambda = 1.0$), while at strong coupling ($\lambda = 0.6$) the E representation result is somewhat higher in energy.

This pattern of results is correlated with the relative quality of the variational wave functions used. Previous experience with the GRW algorithm suggested that the results obtained are insensitive to the choice of guiding function, as long as a sensible choice is made. In the present example, however, we seem to find that a better choice of guiding wave function also results in a better result for the "exact" energy. Ideally, one would like to see as a function of trial state "quality" a sharp separation in energy between those cases where convergence to the same state (the exact ground state) occurs, and other cases where the trial state is so poor that the random walk fails to converge to the correct distribution. Our results seem to indicate that no such sharp separation exists, at least for the lattice gauge theories we consider.

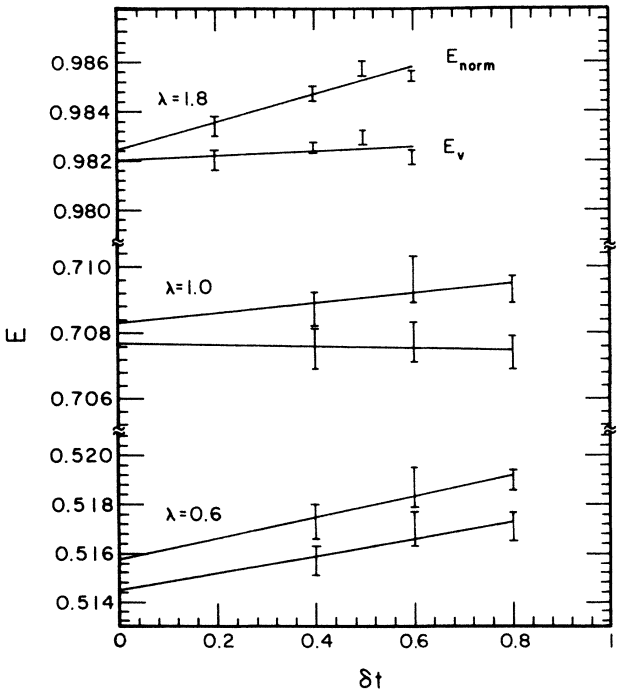

FIG. 2. Extrapolation to $\delta t = 0$ of the ground-state energies obtained with the GRW algorithm in the n basis. E_V and E_{norm} are calculated from the RHS of Eqs. (4.14) and (4.15), respectively.

V. VARIATIONAL CALCULATION OF THE INTERQUARK POTENTIAL

In Monte Carlo calculations based on the Lagrangian formulation of lattice gauge theory, the potential between two static quarks is extracted from measurements of large Wilson loops. As was discussed in Sec. II, an attractive feature of the Hamiltonian formulation is that it allows the interquark potential to be calculated directly as an excitation energy, the difference between the energies of the lowest eigenstates in the vacuum and $q\bar{q}$ subspaces. We will describe below a physically appealing and efficient variational method for estimating this excitation energy. While the variational (as well as the exact) computation of glueball energies is complicated by the need to preserve orthogonality to the vacuum, there are no such problems for the $q\bar{q}$ state: the gauge transformation properties of this state imply that orthogonality is automatically satisfied. We will formulate the variational scheme here specifically for U(1) in $d = 2$ dimensions and hope to describe the generalization to $d = 3$ and to the non-Abelian case in a future publication.

The Hilbert space for the gauge field sector of the $q\bar{q}$ system is spanned by states of the form (2.3), which suggests making the following variational ansatz for the $q\bar{q}$ wave function:

$$|\Phi_{q\bar{q}}\rangle = F_+ |\Psi_0\rangle , \quad F_+ = \sum_{\text{paths } i} W(i) P_+(i) . \tag{5.1}$$

Here, $|\Psi_0\rangle$ denotes (in a basis-independent notation) the exact gauge-invariant vacuum, and F_+ is a weighted sum over all possible path operators $P_+(i)$. To make the ansatz (5.1) tractable, some approximation for the weight $W(i)$ is needed. We feel that a very simple, and yet adequate, choice is to take $W(i)$ dependent only on the length L of the path. Furthermore, it seems reasonable to assume that $W(L)$ decreases exponentially with L:

$$W(L) = \exp(-\alpha L) . \tag{5.2}$$

Given the variational ansatz (5.1), we could now in principle go ahead and calculate $V(R)$ by subtracting the energy of the vacuum, $\epsilon(0)$, from the energy of the $q\bar{q}$ state, $\epsilon(R)$. However, since $\epsilon(R)$ and $\epsilon(0)$ are computed stochastically, such a direct evaluation suffers greatly from statistical imprecision. (Note that both energies grow linearly with the volume of the lattice, while their difference is independent of lattice size and hence small.)

The statistical noise arising from fluctuations in the vacuum energy can be eliminated by expressing $V(R)$ as

$$V(R) = \epsilon(R) - \epsilon(0) = \frac{\langle \Psi_0 | F_-[H, F_+] | \Psi_0 \rangle}{\langle \Psi_0 | F_- F_+ | \Psi_0 \rangle}$$

$$= \frac{\langle \Psi_0 | [F_-, [H, F_+]] | \Psi_0 \rangle}{2 \langle \Psi_0 | F_- F_+ | \Psi_0 \rangle} , \tag{5.3}$$

where we have used the fact that $|\Psi_0\rangle$ is the *exact* vacuum state. The commutator in Eq. (5.3) has the effect of explicitly canceling all "disconnected" contributions to $V(R)$ (disconnected from the "sum-over-paths" operator F_+ and its adjoint, F_-).

To evaluate $[F_-,[H,F_+]]$ we need to work out the double commutator $[P_-(j),[H,P_+(i)]]$ for any pair of paths i and j. Only $H_{\rm elec}$ contributes to this double commutator because $H_{\rm magn}$ and P_+ commute. Furthermore, the factors $e^{\pm i\phi_l}$ appearing in the definition (2.3) are eigenfunctions of the electric-field operator. Evaluation of the double commutator therefore yields $P_-(j)P_+(i)$ multiplied by a c number. This c number is given by the number of links traversed by both i and j in the same direction, minus the number of links traversed by both i and j in the opposite direction. We refer to this quantity as the "intersection" of path i with path j and denote it by $L_{i\cap j}$.

Expression (5.3) for $V(R)$ can now be written as

$$V(R)=\frac{1}{2}\frac{\sum_{ij} L_{i\cap j}Z_{ij}}{\sum_{ij} Z_{ij}}\ , \tag{5.4a}$$

$$Z_{ij}=W(i)W(j)\langle\Psi_0|P_-(j)P_+(i)|\Psi_0\rangle\ , \tag{5.4b}$$

$$\langle\Psi_0|P_-(j)P_+(i)|\Psi_0\rangle=\sum_n \Psi_0(n+i-j)\Psi_0(n)\ . \tag{5.4c}$$

Here, $\Psi_0(n)$ stands for the vacuum wave function as represented in the electric-field basis (n basis) introduced earlier, and $n+i-j$ denotes the configuration obtained by incrementing n in a directed sense on all links contained in path i and decrementing n on all links contained in path j. [Note that the operation of adding i and subtracting j leads to a configuration which again satisfies Gauss's law, $\nabla\cdot(n+i-j)_s=0$.]

Equation (5.4) suggests a physically appealing and efficient algorithm for evaluating $V(R)$ in the present variational framework: use a stochastic method to generate pairs of paths i and j distributed according to Z_{ij}, and then average $L_{i\cap j}$ over these pairs to obtain $V(R)$. We observe that a proper treatment of (5.4) requires an algorithm that samples configurations n from the product $\Psi_0(n+i-j)\Psi_0(n)$, with Ψ_0 the exact vacuum wave function. This might be possible using a generalization of the method described in Sec. IV. However, we chose to simplify the problem even further at this stage and approximate Ψ_0 by an optimized variational wave function, Φ_0. This means that the value of $V(R)$ computed from Eq. (5.4) is no longer a rigorous upper bound on the potential. However, one might still expect that sensible choices for Φ_0 lead to sensible results for $V(R)$.

We have used the following ansatz for Φ_0:

$$\Phi_0(n)=\prod_p I_{m_p}(\beta)\times\prod_l I_{n_l}(\gamma)\ , \tag{5.5}$$

where β and γ are variational parameters, and m is the solution of $n_l=(\nabla\times m)_l$. (Recall that the solution of this equation is unique within an overall additive constant for $d=2$.) Our motivation for choosing the wave function (5.5) becomes evident when the modified Bessel functions are replaced by their asymptotic forms for large arguments:

$$\Phi_0(n)\propto\exp\left[-\frac{1}{2\beta}\sum_p m_p^2-\frac{1}{2\gamma}\sum_l n_l^2\right]\ . \tag{5.6}$$

For a single closed loop of electric flux, this reduces to

$$\Phi_0(n)\propto e^{-(A/\beta+L/\gamma)/2}\ , \tag{5.7}$$

where A is the area of the loop and L is its perimeter. The wave function (5.5) thus combines the attributes of confinement (area dependence) with aspects of long-range order (perimeter dependence). For a given value of the coupling λ, β and γ are determined by minimizing the variational energy: $E_V=\langle\Phi_0|H|\Phi_0\rangle/\langle\Phi_0|\Phi_0\rangle$. ($E_V$ is evaluated stochastically using the standard techniques reviewed in Sec. IV.)

Given an optimal variational approximation to the vacuum, we sample the function Z_{ij}, Eq. (5.4b), by performing a random walk in the space of variables i, j, and n. Using the standard Metropolis algorithm, i is updated according to the weight $W(i)\Phi_0(n+i-j)$, j according to $W(j)\Phi_0(n+i-j)$, and n according to $\Phi_0(n+i-j)\Phi_0(n)$. At certain regular intervals, the random walk is interrupted to measure the intersection $L_{i\cap j}$.

Some qualitative properties of the potential $V(R)$ can be anticipated at this point. In the strong-coupling limit ($\lambda\to 0$), the system prefers the paths i and j to be straight lines connecting the two sources. This gives $V(R)=\frac{1}{2}\langle L_{i\cap j}\rangle\simeq\frac{1}{2}R$ for this limit. As λ increases the paths begin to fluctuate, and these fluctuations become less and less correlated as the number of electric-flux excitations in the vacuum grows. The result is a gradual decrease in the average intersection and, therefore, a gradual decrease in $V(R)$.

We now turn to the discussion of our numerical results. Optimization of the variational parameters for the vacuum wave function (5.5) gave $(\beta,\gamma)=(0.66,11.94)$, $(0.89,3.68)$ and $(0.82,2.76)$ for $\lambda=0.6$, 1.2, and 1.8, respectively.[17] The corresponding vacuum energies are 0.556, 1.038, and 1.471 (with errors only in the fourth decimal), in very close agreement with exact results.[9] The lattices used in our calculations were of size 8×8 for $\lambda=0.6$ and 1.2, and of size 12×12 for $\lambda=1.8$. We typically generated 4000 configurations to compute the average intersection $L_{i\cap j}$. For the 12×12 lattice, each point in the potential required somewhat less than 4 h of CPU time on a VAX 11/750.

Results for the interquark potential $V(R)$ are shown in Fig. 3. At $\lambda=0.6$ the potential is exactly linear, but it is only imperfectly so for $\lambda=1.2$. At $\lambda=1.8$ the linear dependence sets in only for $R\geq 3$, with a dependence weaker than linear (logarithmic?) for $R\leq 3$. We interpret this as the onset of Coulombic behavior at short distances. Values for the string tension have been extracted by making a least-squares linear fit to the data for $V(R)$. For $\lambda=1.2$ only the points for $R\geq 2$ were used in the fit, and for $\lambda=1.8$ only those for $R\geq 3$. The resulting values are displayed in Fig. 4, together with the strong-coupling result and the prediction of Suranyi's weak-coupling variational calculation.[18] (We have taken out a trivial factor g^2

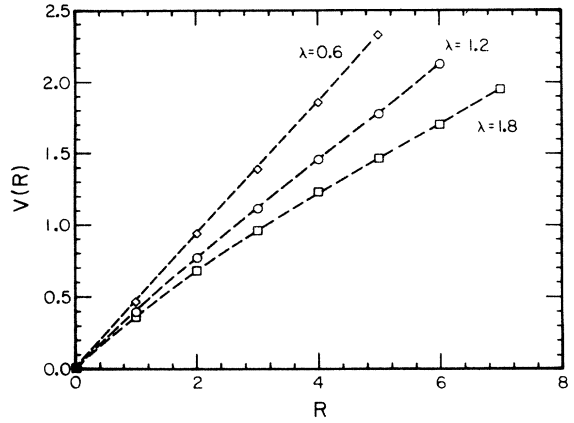

FIG. 3. The potential $V(R)$ between two static sources as a function of separation R. The various points correspond to $\lambda = 0.6$ (diamonds), $\lambda = 1.2$ (circles), and $\lambda = 1.8$ (squares); they have been connected by dashed lines to guide the eye. Statistical errors are roughly equal to the size of the symbols used.

$= \lambda^{-1/2}$ which just sets the overall energy scale.) The points deep in the strong-coupling regime with large error bars are results obtained by DeGrand and Potvin.[9] We observe that our values for the string tension drop considerably (by more than a factor of 2) over the region of coupling strengths considered, but the decrease is less dramatic than would have been expected from Suranyi's calculation.

It is not entirely clear to us whether the difference in results means that the variational ansatz (5.2) is inadequate, or that Suranyi's estimate becomes valid only at $\lambda \gg 1$. It should be noted, however, that our choice of vacuum wave function is rather different from Suranyi's, who uses periodicized harmonic-oscillator wave functions. We found that $V(R)$ is quite sensitive to the structure of Φ_0 when λ is large. For example, a pure independent-link trial function yields at $\lambda = 1.2$ a value for the string tension which is by about a factor of 2 smaller than the result

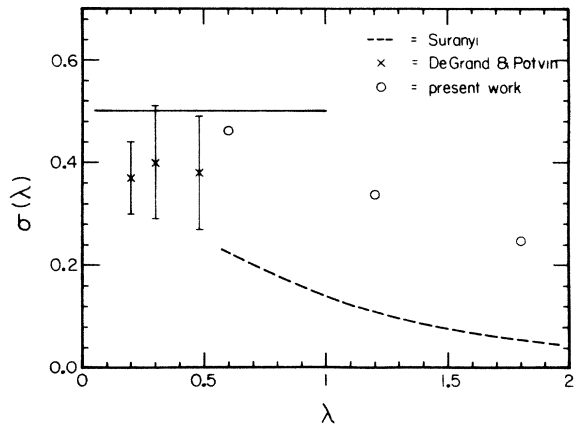

FIG. 4. Results for the string tension, $\sigma(\lambda)$, as calculated from the curves given in Fig. 3. Our results are represented by circles, with statistical errors that are roughly equal to the symbol size used. Crosses correspond to results obtained by DeGrand and Potvin. The dashed line is a weak-coupling variational estimate due to Suranyi.

given in Fig. 4. (The actual system prefers a Φ_0 with a significant independent-plaquette component; see the values for β given above.) Finally, we would like to emphasize again that our results do not set a rigorous upper bound on $V(R)$ as we have approximated the true vacuum Ψ_0 by the trial state Φ_0, Eq. (5.5).

VI. CONCLUSIONS

In this paper, we have studied the Hamiltonian formulation of U(1) lattice gauge theory in the electric-field (E) representation. Our choice of representation was motivated by the fact that the U(1) ground-state wave function in the presence of static sources is complex in the usual vector potential representation, but real and positive in the E representation. We found that there exist (at least) two distinct electric-field bases that are useful for applications: the n and m bases. The first of these is defined by integer electric-field strengths on links and is orthogonal and complete in the total Hilbert space; gauge invariance is enforced by imposing the constraint $\nabla \cdot n = 0$ for all sites. In contrast, the m basis is defined by integers on plaquettes. It is explicitly gauge invariant, but suffers from the drawback of being nonorthogonal and overcomplete. In fact, almost all states in the m basis are unphysical, or redundant.

We have presented a novel variational scheme for calculating the potential $V(R)$ between two static sources. It is based on the physical picture of a string of electric flux connecting the two sources, fluctuating within the vacuum of the theory. The method uses a double-commutator formalism that cancels explicitly all disconnected vacuum contributions and allows $V(R)$ to be computed with high statistical precision. Although it provides only a variational estimate, we feel that this method holds much promise for future applications, including the calculation of potential energies for more complex source configurations such as $q^2\bar{q}^2$, etc.

The calculations for the U(1) gauge group presented here are just an intermediate step toward our eventual goal of treating non-Abelian theories. Let us sketch briefly how to extend the discussion of Sec. III to the non-Abelian case. As before, we find that there exist two different electric-field bases. The non-Abelian analog of the m basis is composed of functions $\langle U \mid m \rangle$ of the form

$$\langle U \mid m \rangle = \prod_p \chi_{m_p}(U_p) . \tag{6.1}$$

Here, $\chi_m(U)$ denotes the character of the gauge group in the irreducible representation labeled by quantum numbers m. The basis functions (6.1) are manifestly gauge invariant, due to the invariance property of characters, but they again suffer from problems related to nonorthogonality and redundancy. Unfortunately, the problems are now much more severe than in the U(1) case because the dependence of the overlap kernel $\langle m' \mid m \rangle$ on m and m' is generally very complicated.

The non-Abelian analog of the n basis is defined by the functions

$$\langle U \mid n \rangle = \prod_l D^{n_l}_{a_l b_l}(U_l) , \tag{6.2}$$

where $D^n_{ab}(U)$ are the representation matrices of the gauge group. Gauge invariance is imposed by considering only linear combinations of these functions that couple the $2d$ matrices touching a given site to a scalar. Several workers in the field have expressed fear at the "forbidding prospect"[9] of implementing such a procedure, but it appears to us as straightforward; for the SU(2) gauge group, it becomes the well-understood problem of coupling $2d$ angular momenta to a singlet.

Having decided on a coupling scheme, we must then evaluate matrix elements of the Hamiltonian in the coupled basis. Matrix elements of the electric part of the Hamiltonian are trivial, as H_{elec} is simply a sum of quadratic Casimir invariants, one invariant for each link. The magnetic term has more complicated matrix elements, which can be written as a product of group recoupling coefficients ($6j$ symbols). An important point here is that, since H_{magn} is placed in the fundamental representation (FR) of the gauge group ($H_{\text{magn}} \propto \sum_p \text{tr} U_p$), at least one entry in each $6j$ symbol must be the FR. The relevant $6j$ symbols therefore can be precomputed and stored in a table of relatively small size. Closed algebraic expressions for the SU(2) $6j$ symbols have been given by Racah.[19] A major complication, as compared to the Abelian case, is that not all off-diagonal matrix elements of H_{magn} are of the same sign, and so the relative phases of the components of a good trial wave function are not obvious. This, and other questions related to implementing our approach for non-Abelian theories, are currently being investigated.

ACKNOWLEDGMENTS

This work was supported in part by the National Science Foundation, Grants Nos. PHY82-07332 and PHY83-15500. E.A.U. and M.R.Z. acknowledge support by Caltech Bantrell and Weingart Research Fellowships, respectively.

APPENDIX: INDEPENDENT-LINK WAVE FUNCTION IN THE A REPRESENTATION

We transform the independent-link wave function $\Phi(n)$, Eq. (3.10), to the vector potential basis. By eliminating the gauge constraints $(\nabla \cdot n)_s = 0$ through the introduction of auxiliary integration variables μ_s, $0 \le \mu_s < 2\pi$, we can write $\Phi(\phi)$ as

$$\Phi(\phi) = \sum_n \int d[\mu] \left[\prod_l I_{n_l}(\beta) \right] \exp\left[i \sum_l n_l \phi_l \right] \times \exp\left[i \sum_s (\nabla \cdot n)_s \mu_s \right] . \tag{A1}$$

The next step is to make a lattice "integration by parts,"

$$\sum_s (\nabla \cdot n)_s \mu_s = - \sum_l (\nabla \mu)_l n_l , \tag{A2}$$

where $(\nabla \mu)_l$ means the difference between the values of μ_s at the two sites bounding the link l. The sum over n can now be performed to give

$$\Phi(\phi) = \int_{-\pi}^{\pi} d[\mu] \exp\left[\beta \sum_l \cos[(\nabla \mu)_l - \phi_l] \right] . \tag{A3}$$

In the weak-coupling limit, β becomes large and it is a valid approximation to expand the cosine:

$$\cos[(\nabla \mu)_l - \phi_l] \simeq 1 - \tfrac{1}{2}[(\nabla \mu)_l - \phi_l]^2 . \tag{A4}$$

Performing another integration by parts we find

$$\Phi(\phi) \propto \int_{-\pi}^{\pi} d[\mu] \exp\left[\frac{\beta}{2} \left[\sum_s \mu_s (\nabla^2 \mu)_s - 2 \sum_s \mu_s (\nabla \cdot \phi)_s - \sum_l \phi_l^2 \right] \right] . \tag{A5}$$

Since the integral is dominated by a narrow range of values of μ, we can extend the limits of integration to infinity, thereby reducing the expression (A5) to a Gaussian integral which is evaluated by completing the square:

$$\Phi(\phi) \propto \exp\left[-\frac{\beta}{2} \left[\sum_l \phi_l^2 + \sum_s (\nabla \cdot \phi)_s [(\nabla^2)^{-1} (\nabla \cdot \phi)]_s \right] \right] . \tag{A6}$$

In momentum space, the exponent of (A6) in the continuum approximation is given by

$$-\frac{\beta}{2} \sum_k \left[|\phi|^2 - \frac{|k \cdot \phi|^2}{k^2} \right] = -\frac{\beta}{2} \sum_k \frac{|k \times \phi|^2}{k^2} , \tag{A7}$$

where reciprocal lattice cross and dot products are understood. In coordinate space, $k \times \phi$ is simply the lattice curl of ϕ and, thus, the wave function in the A representation for $d = 3$ can be written as

$$\Phi(\phi) \propto \exp\left[-\frac{\beta}{2} \sum_{pp'} \frac{\psi_p \psi_{p'}}{|p - p'|} \right] , \tag{A8}$$

where $|p - p'|$ is the distance between the plaquettes p and p'. Equation (A8) makes manifest the gauge invariance of Φ, as well as the presence of long-range correlations between the plaquette variables ψ_p.

*Deceased.
[1]M. Creutz, L. Jacobs, and C. Rebbi, Phys. Rev. D **20**, 1915 (1979).
[2]H. Hamber and G. Parisi, Phys. Rev. Lett. **47**, 1792 (1981).
[3]F. Fucito, G. Martinelli, C. Omero, G. Parisi, R. Petronzio, and R. Rapuano, Nucl. Phys. **B210**, 407 (1982).
[4]J. Kogut and L. Susskind, Phys. Rev. D **11**, 395 (1975).
[5]S.A. Chin, J.W. Negele, and S.E. Koonin, Ann. Phys. (N.Y.) **157**, 140 (1984).
[6]S.A. Chin, O.S. van Roosmalen, E.A. Umland, and S.E. Koonin, Phys. Rev. D **31**, 3201 (1985).
[7]D.W. Heys and D.R. Stump, Phys. Rev. D **28**, 2067 (1983).
[8]D.W. Heys and D.R. Stump, Nucl. Phys. **B257**, 19 (1985).
[9]T.A. DeGrand and J. Potvin, Phys. Rev. D **31**, 871 (1985).
[10]A. Duncan and R. Roskies, Phys. Rev. D **31**, 364 (1985).
[11]A.M. Polyakov, Phys. Lett. **72B**, 477 (1978).
[12]E. Fradkin and L. Susskind, Phys. Rev. D **17**, 2637 (1978).
[13]S.D. Drell, H.R. Quinn, B. Svetitsky, and M. Weinstein, Phys. Rev. D **19**, 619 (1979).
[14]G. Bhanot, C.B. Lang, and C. Rebbi, Comput. Phys. Commun. **25**, 275 (1982).
[15]N. Metropolis, A.W. Rosenbluth, M.N. Rosenbluth, A.H. Teller, and E. Teller, J. Chem. Phys. **21**, 1087 (1953).
[16]S.A. Chin (private communication).
[17]Actually, for $\lambda = 0.6$ the parameter set is ill determined. This can be understood by observing that in the strong-coupling limit the vacuum is a dilute system of single-plaquette excitations, whose total perimeter L and area A are related, $L = 4A$. The wave function (5.5) therefore depends on only a *single* combination of the parameters β and γ. We have checked that the indeterminacy in β and γ for small λ has no effect on the value of $V(R)$. For example, the set $(\beta,\gamma) = (0.93,6.32)$ yields, within statistical errors, the same results as that given in the text.
[18]N. Suranyi, Nucl. Phys. **B225**, 77 (1983).
[19]G. Racah, Phys. Rev. **62**, 438 (1942).